A Simple Friction and Diffusion Scheme for Planetary Geostrophic Basin Models

R. M. SAMELSON

Woods Hole Oceanographic Institution, Woods Hole, Massachusetts

GEOFFREY K. VALLIS

University of California, Santa Cruz, California

19 July 1994 and 16 April 1996

ABSTRACT

A simple friction and diffusion scheme is proposed for use with the time-dependent planetary geostrophic equations, which in their proper asymptotic form cannot be solved in a closed basin. The resulting set of equations admits boundary conditions of no-normal flow and no-normal heat flux at all rigid boundaries, is amenable to efficient numerical solution, and may be solved with small heat (and salt) diffusivities. The scheme is formally a minor modification of several others that have recently been proposed but differs in significant details. Friction is represented by linear drag in the horizontal momentum equations, while the hydrostatic balance is retained exactly. The Laplacian vertical and horizontal heat (and salt) diffusion are supplemented by biharmonic horizontal diffusion. The latter is necessary in order that the smoothness of the solution can be maintained up to and along the boundary, which is particularly important because the no-normal-flow condition is enforced as a differential equation that must be solved along the boundary. The equations support a frictional western boundary current that is nearly adiabatic.

1. Introduction

Standard scaling analysis for gyre-scale oceanic motion leads to the planetary geostrophic equations, the adiabatic and inviscid (''ideal'') form of the ''thermocline'' or ''Phillips type II'' equations (Robinson and Stommel 1959; Welander 1959; Phillips 1963; Pedlosky 1984). In their simplest dimensionless β-plane form, these equations are

$$-fv + p_x = 0 \tag{1.1}$$

$$fu + p_y = 0 \tag{1.2}$$

$$p_z - T = 0 \tag{1.3}$$

$$u_x + v_y + w_z = 0 \tag{1.4}$$

$$T_t + uT_x + vT_y + wT_z = 0. \tag{1.5}$$

A diffusive term is commonly appended to (1.5) as a first-order representation of the effect of microscale turbulent mixing, giving

$$T_t + uT_x + vT_y + wT_z = \kappa_v T_{zz}. \tag{1.5$'$}$$

In these equations, (u, v, w) are the (x, y, z)-components of velocity, t is time, p is pressure, T is temperature (taken equal to the negative of density), and subscripts x, y, z, and t denote partial derivatives. The Coriolis parameter $f = f_0 + \beta y$, where f_0 and β are constants.

The underlying structure of this set of equations is perhaps most apparent if, following Welander (1971), the scalar field $M(x, y, z, t)$ is defined by

$$M_z = p. \tag{1.6}$$

From (1.1)–(1.4) and (1.6), the temperature T and velocities (u, v, w) may be written as derivatives of M,

$$T = M_{zz}, \qquad u = -f^{-1}M_{zy},$$

$$v = f^{-1}M_{zx}, \qquad w = \beta f^{-2}M_x. \tag{1.7}$$

Using these in (1.5′) enables the system to be written as a single evolution equation for M,

$$M_{zzt} - f^{-1}M_{zy}M_{zzx} + f^{-1}M_{zx}M_{zzy} + \beta f^{-2}M_x M_{zzz} = \kappa_v M_{zzzz}. \tag{1.8}$$

This shows that, away from lateral boundaries, (1.1)–(1.5′) are in principle sufficient to determine the evolution of the flow, when appropriate top and bottom boundary conditions on M are given.

However, these equations, even with the diffusive term of (1.5′), cannot generally be solved in a closed basin. Imposing appropriate boundary conditions leads to the formation of discontinuities and loss of differ-

Corresponding author address: Dr. Roger M. Samelson, WHOI MS#21, Woods Hole, MA 02543-1541.

entiability at lateral boundaries. When the fluid is confined by vertical lateral boundaries, as in the simplest models of ocean basins, the no-normal-flow condition requires, by (1.1)–(1.3), that the pressure and density be constant at fixed levels along the lateral boundaries. If the geostrophic no-normal-flow condition is imposed along the eastern boundary, it is easily seen from the vertically integrated Sverdrup vorticity balance that this results in a pressure discontinuity at the western boundary at any latitude with nonzero zonally averaged Ekman pumping into the interior (e.g., Stommel 1948; Pedlosky 1987). Thus, (1.1)–(1.5′), or their layer equivalents, can be solved only on restricted domains that are isolated from some or all lateral boundaries. That approach has produced many important insights (e.g., Needler 1967; Welander 1971; Luyten et al. 1983; Huang 1988), but the inability of the equations to represent the circulation in a closed basin has limited their utility in the study of the large-scale circulation.

An additional difficulty with the time-dependent equations was pointed out by Colin de Verdiere (1986), who showed that arbitrarily short linear disturbances will grow arbitrarily fast when the flow becomes baroclinically unstable. This tendency for unphysical growth at small scales must also be overcome if the time-dependent equations are to be solved numerically.

Here a simple friction and diffusion scheme is proposed that alleviates these difficulties. It generally follows the approach of Salmon (1986), yet maintains hydrostatic balance. The resulting set of equations forms an appealingly simple, computationally efficient, idealized model of the large-scale ocean circulation, in which the effects of motions at scales between the turbulent microscale and the planetary scale are minimized, and which may be solved with small turbulent diffusivities. We briefly present some illustrative numerical solutions of these equations. The thermocline structure that arises in solutions of these equations in a closed basin is analyzed by Samelson and Vallis (1997). That analysis illustrates how two differing theoretical models of the subtropical thermocline, the adiabatic ''ventilated thermocline'' theory (Luyten et al. 1983) and the intrinsically diffusive ''internal boundary layer'' thermocline theory (Stommel and Webster 1962; Salmon 1990) may be related in the small-diffusion limit.

2. A simple friction and diffusion scheme

The friction and diffusion scheme that we propose as a minimal supplement to the planetary geostrophic equations consists of linear drag in the horizontal momentum equations and a combination of Laplacian and biharmonic horizontal diffusion in the thermodynamic equation, so that the full dimensionless equations are

$$-fv + p_x = -\epsilon u \tag{2.1}$$

$$fu + p_y = -\epsilon v \tag{2.2}$$

$$p_z - T = 0 \tag{2.3}$$

$$u_x + v_y + w_z = 0 \tag{2.4}$$

$$T_t + uT_x + vT_y + wT_z = \kappa_v T_{zz} + \kappa_h \Delta_h T - \lambda \Delta_h^2 T, \tag{2.5}$$

where

$$\Delta_h = \frac{\partial^2}{\partial x^2} + \frac{\partial^2}{\partial y^2}. \tag{2.6}$$

Hydrostatic balance and incompressibility are retained. The coefficients ϵ, κ_h, λ are small and positive.

The linear drag (ϵ) in the horizontal momentum equations has appeared in related schemes proposed by previous authors (Killworth 1985; Salmon 1986, 1990; Zhang, et al. 1992; Winton and Sarachik 1993) and allows the no-normal-flow condition to be applied to the barotropic flow. In the homogeneous case, it is essentially equivalent to the bottom friction invoked by Stommel (1948). If the stratification T_z does not vanish anywhere, it also allows the no-normal-flow condition to be applied to the depth-dependent flow. As shown below, it does not allow this if horizontal temperature gradients dominate vertical gradients at the boundary.

The Laplacian (κ_h) and biharmonic (λ) horizontal diffusion are familiar features of numerical ocean models, though normally only one or the other is used, not both as here. Often, biharmonic diffusivities are used as ''numerical filters'' to provide scale-selective damping of interior variance (e.g., Cox 1985). In the present case, the horizontal diffusion is used specifically to smooth the solution at the lateral boundaries as well as in the interior. We show below that this is necessary. For both physical and mathematical reasons, the horizontal diffusivities κ_h and λ must be chosen small enough (relative to κ_v) that the net diapycnal fluxes are dominated by vertical diffusion, but large enough that the lateral boundary layers can be resolved.

The frictional-geostrophic relations (2.1) and (2.2) may be inverted locally for the horizontal velocities, giving

$$u = -\gamma(\epsilon p_x + f p_y), \quad v = \gamma(f p_x - \epsilon p_y), \tag{2.7}$$

where $\gamma = (f^2 + \epsilon^2)^{-1}$. The vertical derivative of (2.7) yields the frictional-geostrophic analog of the thermal wind relations,

$$u_z = -\gamma(\epsilon T_x + f T_y), \quad v_z = \gamma(f T_x - \epsilon T_y). \tag{2.8}$$

Consequently, the no-normal-flow boundary condition must be imposed as a boundary condition on the temperature,

$$\epsilon T_n + f T_s = 0, \tag{2.9}$$

where the subscripts n and s denote the normal and right-handed tangential derivatives, respectively. The no-heat-flux condition at lateral boundaries takes the form

$$-\kappa_h T_n + \lambda \Delta_h T_n = 0. \tag{2.10}$$

The no-normal-flow condition (2.9) is a differential equation that must be solved around the boundary, simultaneously with the interior equations (2.1)–(2.5).

The generalization to $\epsilon > 0$ of Welander's (1971) argument shows that the system (2.1)–(2.5) may be written as a single equation in the dependent variable M,

$$\begin{aligned} M_{zzt} - \gamma(fM_{zy} + \epsilon M_{zx})M_{zzx} + \gamma(fM_{zx} - \epsilon M_{zy})M_{zzy} \\ + [\mathcal{H}(M) + W_0]M_{zzz} \\ = \kappa_v M_{zzzz} + \kappa_h \Delta_h M_{zz} - \lambda \Delta_h^2 M_{zz}, \end{aligned} \tag{2.11}$$

where as before

$$M_z = p, \tag{2.12}$$

$\mathcal{H}$ is defined below by (3.7), and the additional boundary condition $M(z = 0) = 0$ has been imposed. The upper boundary condition on M is $M(z = 1) = P$, where P is the barotropic pressure,

$$P = \int_0^1 p \, dz. \tag{2.13}$$

Here P is obtained from the elliptic equation

$$\mathcal{H}(P) = W_1 - W_0, \tag{2.14}$$

where W_1 and W_0 are the imposed vertical velocities at the top and bottom, respectively, and (2.14) is solved subject to the vertically integrated no-normal-flow condition

$$\epsilon P_n + f P_s = 0 \tag{2.15}$$

at lateral boundaries. This shows explicitly the intrinsic simplicity of the present equations. In addition, it shows directly that the horizontal differential order of the interior equations is four, equal to the number of imposed boundary conditions (no-normal-flow and no-normal-heat-flux at each pair of opposing boundaries), independent of any properties of the solution.

3. Boundary discontinuities

When the fluid adjacent to the boundary is locally unstratified ($T_z = 0$) but has horizontal temperature gradients, imposing the boundary condition (2.9) may lead immediately to the formation of discontinuities at the boundary if $\kappa_h = \lambda = 0$ in (2.1)–(2.5). This can be seen as follows: Consider an initial value problem for (2.1)–(2.5), with $\kappa_h = \lambda = 0$, in which the initial base field T_0 is unstratified along the northern boundary $y = 1$; for example,

$$T_0 = \epsilon x + f_0 y + \frac{1}{2}\beta y^2 \tag{3.1}$$

with $P = 0$ for simplicity. This T_0 is not a steady-state solution itself, but it does satisfy the no-normal-flow condition (2.9). Small disturbances $T' = T - T_0$ to this state will initially evolve according to the linearization of (2.5) about T_0, which (with $P' = 0$) is

$$\begin{aligned} T'_t - \left(z - \frac{1}{2}\right)T'_x + \epsilon u' + f v' \\ = \kappa_v T'_{zz} + \epsilon\left(z - \frac{1}{2}\right). \end{aligned} \tag{3.2}$$

From this equation and the no-normal-flow condition (2.9), an equation follows for the initial evolution of the vertical shear of the normal flow at the boundary $y = 1$,

$$v'_{zt} = 2\epsilon f \gamma v'_y \qquad \text{on} \quad y = 1. \tag{3.3}$$

Thus, the evolution equation for T will be consistent with the maintenance of the no-normal-flow condition only if the normal horizontal convergence v'_y of the initial linear disturbance vanishes, which it need not. In other words, if the no-normal-flow condition is imposed, a discontinuity will immediately arise at the boundary.

The origin of this difficulty can be seen by linearizing the equations about a state of uniform stratification $T_z = G > 0$, where G is a constant. To allow comparison also with the nonhydrostatic scheme proposed by Salmon (1986, 1990), we replace (2.3) by the more general equation

$$p_z - T = -rw. \tag{3.4}$$

The hydrostatic equation (2.3) may be recovered by setting $r = 0$. The equations considered are (2.1), (2.2), (3.4), (2.4), with (2.5) replaced by the steady linearized equation (here μ is a thermal damping coefficient)

$$wG = \mathcal{L}(T) = \kappa_v T_{zz} + \kappa_h \Delta_h T - \lambda \Delta_h^2 T - \mu T. \tag{3.5}$$

From (2.7), the continuity equation (2.4) may be written

$$\mathcal{H}(p) = w_z, \tag{3.6}$$

where $\mathcal{H}$ is defined by

$$\begin{aligned} \mathcal{H}(\phi) = \epsilon\gamma\Delta_h\phi + (f^2 - \epsilon^2)\gamma^2\beta\phi_x \\ - 2\epsilon f\gamma^2\beta\phi_y. \end{aligned} \tag{3.7}$$

It is then straightforward to eliminate w and p from (3.4), (3.5), and (3.6) to obtain a single equation for T,

$$\mathcal{D}(T) \equiv r\mathcal{H}[\mathcal{L}(T)] + \mathcal{L}(T_{zz}) - G\mathcal{H}(T) = 0 \tag{3.8}$$

or equivalently,

$$\left[\epsilon\gamma\Delta_h + (f^2 - \epsilon^2)\gamma^2\beta\frac{\partial}{\partial x} - 2\epsilon f\gamma^2\beta\frac{\partial}{\partial y}\right]\left[r\left(-\lambda\Delta_h^2 T + \kappa_h\Delta_h T + \kappa_v\frac{\partial^2}{\partial z^2}T - \mu T\right) - GT\right]$$
$$-\lambda\Delta_h^2\frac{\partial^2}{\partial z^2}T + \kappa_h\Delta_h\frac{\partial^2}{\partial z^2}T + \kappa_v\frac{\partial^4}{\partial z^4}T - \mu\frac{\partial^2}{\partial z^2}T = 0. \quad (3.9)$$

Alternatively, w and T may be eliminated from (3.4), (3.5), and (3.6) to obtain a similar equation for p,

$$\mathcal{D}'(p) \equiv r\mathcal{L}[\mathcal{H}(p)] + \mathcal{L}(p_{zz}) - G\mathcal{H}(p) = 0. \quad (3.10)$$

The differential order of the linearized system for various values of the parameters may be deduced by inspection of (3.9). Various choices are considered in the appendix. The result of relevance here is that if $\kappa_h = \lambda = r = 0$, the term of leading horizontal differential order is proportional to $\epsilon G\Delta_h T$. This shows that as long as $\epsilon > 0$ and $G > 0$, the system is second order in x and y, and the no-normal-flow condition (2.9) may be consistently imposed at each pair of opposing lateral boundaries. However, as G approaches zero, the lateral boundary layer thickness will also approach zero. This is consistent with the argument above, which showed that discontinuities can form at the boundary when the stratification vanishes if no explicit horizontal diffusion is included in the hydrostatic case ($r = 0$).

Since the boundary condition (2.9) takes the form of a differential equation, it is important to smooth any discontinuities that arise at the boundary in order to maintain the solvability of the system. This may be achieved by introducing explicit horizontal diffusion. Since the no-normal-flow condition already implies the lateral boundary condition (2.9) on T, Laplacian diffusion alone is insufficient, as it will lead to an unphysical heat flux through the lateral boundaries. This cannot be avoided by reducing the diffusivity to zero at the boundary, because the discontinuity that must be smoothed is itself located at the boundary. A simple and effective solution is to introduce biharmonic diffusion. The no-heat-flux condition at lateral boundaries then takes the form (2.10) and finite diffusivities may be retained at the boundary to prevent the formation of discontinuities there. The combination of Laplacian and biharmonic diffusion also effectively damps the planetary geostrophic short-wave instabilities (Colin de Verdiere 1986) in the interior.

4. Western boundary layer

The barotropic pressure P from the solution of (2.14) has the Stommel (1948) exponential western boundary layer thickness scale ϵ/β. If vertical motion in the boundary layer is small, the same scale will arise naturally for the baroclinic western boundary layer, as may be inferred if (3.6) is written in the form of a vorticity equation,

$$\beta v = fw_z - \epsilon(v_x - u_y), \quad (4.1)$$

since the boundary layer balance will then be between the βv and ϵv_x terms. A systematic difficulty in coarse-grid level-coordinate large-scale circulation models is the generation of unphysical diapycnal fluxes by horizontal diffusion across the tilted isotherms of western boundary currents (Veronis 1975). In the present case, the corresponding fluxes may be substantially reduced by the choice of a specific value of the biharmonic diffusivity λ,

$$\lambda = \lambda_0 \equiv (\epsilon/\beta)^2\kappa_h, \quad (4.2)$$

since exponential variation on the scale $(\lambda/\kappa_h)^{1/2} = \epsilon/\beta$ yields no net horizontal diffusive flux from the combination of Laplacian and biharmonic diffusion, as is easily verified by direct substitution. This in turn is consistent with the assumption of an ϵ/β frictional western boundary layer from the vorticity equation, with weak vertical motion, since the net horizontal advection and net horizontal diffusion should then be separately small in (2.5). This line of reasoning is not a complete boundary layer analysis and should be considered a plausibility argument.

The numerical solutions of (2.1)–(2.5) that we have obtained have a western boundary layer structure that is generally consistent with this argument, as a frictional boundary layer arises that is adiabatic to first order, despite the presence of horizontal diffusion in the equations. On the other hand, we have argued that diffusion must be introduced in part to smooth the solution along the boundaries, and so must play a significant role there. In the next section, a preliminary examination of these details in numerical solutions is discussed. There is a subtle but important point to be emphasized here: since the required diffusive effect may arise only in specific isolated areas, it need not dominate the general structure of the solution (and evidently does not, in the numerical solutions we have examined). The dominant physical mechanism that allows closed circulations to occur is the frictional torque in the western boundary layer. Nonetheless, the diffusive effect is critical in that it maintains the local differentiability of the solution at the boundary and thus the global solvability of the equations.

5. Numerical examples

The critical effect that the additional (biharmonic) horizontal diffusion term can have on the solvability of the equations may be illustrated by comparing a solution of the present equations (2.1)–(2.5) with a solution of

the nonhydrostatic planetary geostrophic equations of Salmon (1990), which are well posed but computationally demanding, and with a hydrostatic numerical result with zero biharmonic diffusivity. In this comparison, the critical diffusive effect occurs at the poleward termination of the western boundary current.

A simple slab Ekman layer with temperature advection was used to set the upper boundary condition on temperature, while the Ekman layer vertical velocity W_E (proportional to wind stress curl) was used to set the boundary condition $w = W_1 = W_E$ on interior vertical velocity at the base of the layer. The barotropic pressure P (which was time independent, since the forcing was steady) was obtained from the solution of (2.14), with $w = W_0 = 0$ imposed at the flat bottom. The model equations, supplemented by a standard convective-adjustment scheme, were then time stepped until the solutions reached equilibrium.

The numerical integration scheme for the nonhydrostatic model followed Salmon (1990). The hydrostatic-biharmonic equations (2.1)–(2.5) were integrated as described by Samelson and Vallis (1997). In the latter case, the pressure field may be obtained from the temperature field from the known barotropic pressure P and the hydrostatic relation (2.3), and the velocity field may then be obtained from the frictional–geostrophic balance relations (2.7) and the continuity equation (2.4). In the former case, a three-dimensional elliptic equation must be solved at each step to obtain the velocity field from the pressure and temperature, and as a result, the computational demand is much greater (by a factor of 16, for the calculations presented here) for the nonhydrostatic model than for the hydrostatic model. In either case, the temperature field may then be stepped forward one time step and the process repeated. The lateral boundary conditions imposed on the temperature field in the hydrostatic model are (2.10) and (2.9), while (2.10) (with $\lambda = 0$) and a condition like (2.15) on the baroclinic pressure are imposed in the nonhydrostatic model. Finite difference representations of (2.10), (2.9), and (2.15) are easily derived, with (2.9) and (2.15) giving cyclic tridiagonal problems that can be solved rapidly by standard matrix methods. The heat flux condition (2.10) with $\lambda > 0$ can be imposed in a simple way if the biharmonic diffusion is coded as an iterated Laplacian (i.e., the discrete Laplacian operator is first applied to the temperature field to obtain $\Delta_h T$, the boundary values are then computed, and finally the Laplacian is applied again to obtain $\Delta_h^2 T$).

For the comparison, we integrated both models with a purely zonal wind stress of the form

$$\tau = \tau_0 f(y)\sin(2\pi y) \tag{5.1}$$

and a surface heat flux proportional to the difference between the Ekman layer temperature and an imposed meridional air temperature T_a that decreased linearly with y. The friction and diffusion coefficients were taken to be large enough (see figure caption for numerical values) that planetary geostrophic baroclinic instabilities (Colin de Verdiere 1986) were damped, and the solutions approached a steady state. The solutions were obtained on $33 \times 33 \times 16$ grids.

The density field at the uppermost interior grid level (just below the surface Ekman layer) from the hydrostatic and nonhydrostatic solutions are shown in Figs. 1a and 1b, respectively. In the interior, the near-surface density is controlled primarily by the surface boundary conditions, and consequently the two solutions are similar. However, the two solutions also place the separation point of the western boundary current (marked by the large meridional density gradient adjacent to the western boundary) at nearly the same latitude, roughly $y = 0.85$. This similarity may be contrasted with the difference that arises if a hydrostatic numerical result is generated in which the biharmonic diffusivity λ is set equal to zero everywhere and (2.10) is ''satisfied'' by reducing the gradient diffusivity κ_h to zero at the lateral boundaries. (For that case, the Laplacian diffusion term was rewritten as the divergence of the gradient flux, as appropriate for a spatially variable diffusivity.) The corresponding density cross section from that computation, shown in Fig. 1c, disagrees with the first two numerical solutions by an order one amount in the northwestern part of the domain. The third computation does not result simply in an ''unsmoothed'' version of the first two density fields, but instead induces a first-order error (with respect to the numerical solution of either well-posed set of equations) in the structure of the solution along the western boundary. This error is evidently induced by the tendency of the unsmoothed equations to generate discontinuities along the boundary when horizontal temperature gradients dominate vertical gradients locally, as illustrated by the linear analysis (3.1)–(3.3) above.

This comparison gives a concrete illustration of two points. First, the agreement of the solutions in Figs. 1a and 1b, which use two fundamentally different (but well posed) schemes, suggests that the common element of these two schemes (the horizontal linear drag) controls the global structure of the western boundary current, while the additional element (the biharmonic diffusion in the hydrostatic case, and the vertical linear drag in the nonhydrostatic case) serves primarily to smooth the solution locally. As argued above, this smoothing is necessary in order to maintain global solvability, but in these solutions at least, it evidently does not directly control the first-order global structure. The similarity of the pressure gradients along the boundary (Fig. 2) in these two solutions supports the conclusion that the same horizontal momentum balance controls the meridional structure of the boundary layer in both cases. Second, the hydrostatic calculation with zero boundary diffusivity demonstrates the subtle breakdown of the solution that can occur if smoothness is not explicitly maintained along the boundary. In that case, a local numerical instability evidently arises in response to the

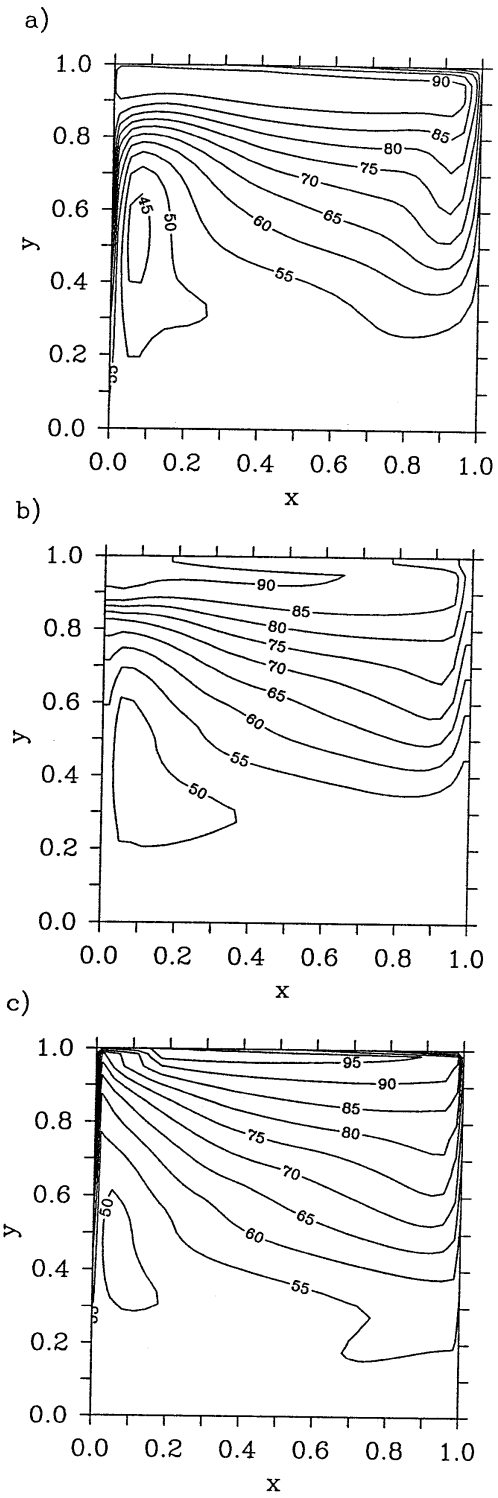

FIG. 1. Density $\rho = -T$ just below the Ekman layer from solutions of (a) the hydrostatic model with biharmonic diffusion, (b) the nonhydrostatic model, and (c) the hydrostatic model with a spatially varying gradient diffusivity that vanishes at the boundary and no biharmonic diffusion. The solutions have $f_0 = f(y = 0.5) = 0.65$, $\beta = 0.6$, $\kappa_v = 0.01$, $\kappa_h = 0.05$, $\epsilon = 0.04$, $\tau_0 = 1/(2\pi)$, $T_a = -100y$. In (a) $\lambda = (\epsilon/\beta)^2\kappa_h$, $r = 0$; in (b) $\lambda = 0$, $r = 0.004$; and in (c) $\lambda = 0$, $r = 0$ and $\kappa_h = 0.05$ in the interior and decreases linearly to zero at the boundary.

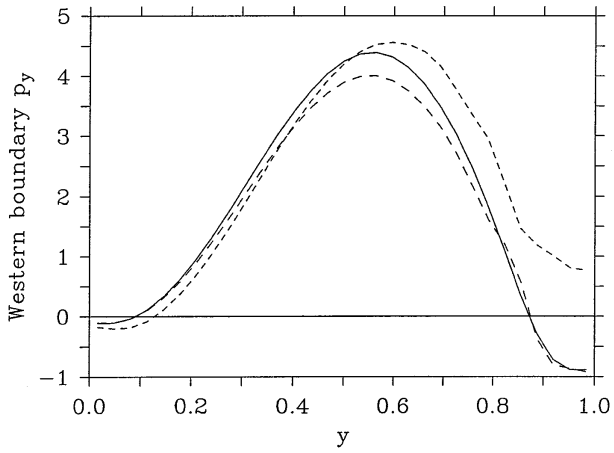

FIG. 2. Pressure gradient p_y along the western boundary from the solutions (a) solid line, (b) long dashes, (c) short dashes in Fig. 1 and at the corresponding depth.

development of the discontinuity at the boundary, and the numerical result is consequently altered in a fundamental way that is related not to the equations purportedly being solved, but to the details of the numerical discretization and implementation. Although the numerical scheme is not fully unstable and still produces results with some recognizable similarities in the interior to the proper solutions, the relation between the numerical results and the specified physical model has essentially been destroyed.

The present comparison can be criticized on the grounds that the nonhydrostatic scheme of Salmon (1990) is itself ad hoc. However, the similarity of the two solutions suggests that neither the interior flow nor the separation of the boundary current is critically dependent on the form of the smoothing. Comparisons with solutions of the primitive equations (Bryan 1969) and the planetary geostrophic equations of Colin de Verdiere (1988, 1989) are complicated by the different boundary conditions on horizontal velocity (no-slip rather than no-normal-flow). In work reported elsewhere (Samelson and Vallis 1997), we compare numerical solutions of the present equations to analytical partial-domain and similarity solutions of the thermocline equations (1.1)–(1.5). There is no indication from these various comparisons and analyses that the higher-order diffusive smoothing has any pathological influence.

Finally, in order to demonstrate that it is possible to integrate the present equations across the equator, we show a solution in a two-hemisphere basin (Fig. 3). Note that the Eqs. (2.1)–(2.5) are not singular at the equator, where $f = 0$, because of the presence of the frictional terms in the horizontal momentum equations. For the solution shown in Fig. 3, the resolution was $65 \times 65 \times 16$ grid points and a stretched vertical grid was used. The domain and the wind forcing are symmetric about the equator, with a single band of tropical easterlies and midlatitude westerlies in each hemisphere, and there is

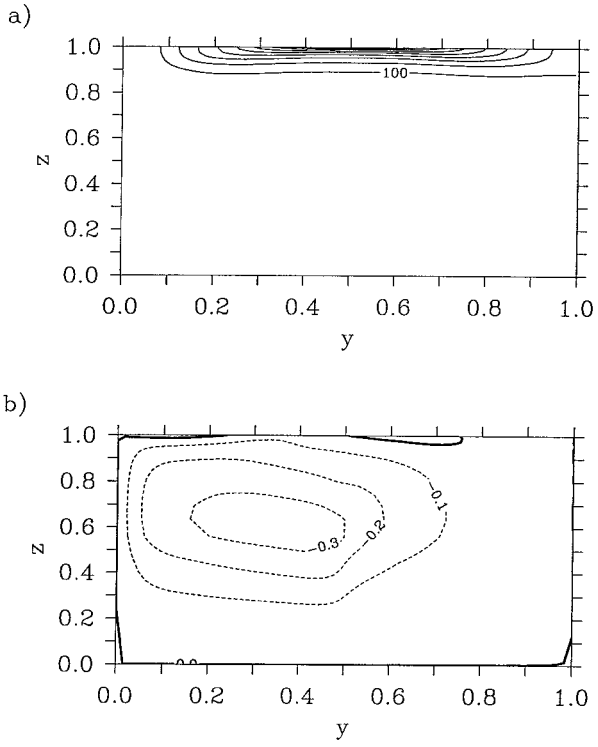

FIG. 3. (a) North–south vertical section of zonally averaged density from a hydrostatic solution in a two-hemisphere basin. The model equator is at $y = 0.5$, and the cooler hemisphere, with the larger meridional temperature gradient, is on the left. This solution has $f_0 = f(y = 0.5) = 0$, $\beta = 3$, $\kappa_v = 0.01$, $\kappa_h = 0.1$, $\lambda = (\epsilon/\beta)^2\kappa_h$, $\epsilon = 0.1$, $\tau_0 = 1/(2\pi)$, $T_a = \{-250(0.5 - y), y < 0.5; -200(y - 0.5), y > 0.5\}$.(b) Meridional overturning streamfunction.

no freshwater forcing. The thermal forcing is weakly asymmetric, with a 5:4 ratio of imposed meridional air temperature gradient in the two hemispheres. The thermocline is strong and shallow at the equator, and deepens and weakens toward both polar boundaries (Fig. 3a). The meridional overturning of the zonally averaged flow is strongly asymmetric and is characterized by a single direct cell (Fig. 3b). Most of the abyss in both hemispheres is filled with the coldest water available; that is, ''bottom water'' is formed from the highest latitudes of the colder hemisphere only. Symmetric thermal forcing leads to a symmetric solution (not shown).

6. Discussion

The necessity for introduction of a higher-order diffusion term in the hydrostatic model with linear drag (2.1)–(2.5) is perhaps counter-intuitive, since it might appear that the original equation (1.5′) could be integrated all the way up to, and along, the lateral boundary, independent of any boundary conditions on T. It is a consequence of the hydrostatic relation that the boundary conditions on pressure and temperature are not independent when the velocity depends locally on the pressure gradient, as is clear when the hydrostatic system is written in the form (1.8) or (2.11). In the presence of stratification, the elliptic behavior of the frictionally driven, hydrostatic vertical velocity that arises through (3.6) is sufficient to supply the necessary (nonlinear) lateral boundary layers without explicit horizontal temperature diffusion, but if the temperature field along the boundary is dominated by horizontal variations, the linear friction is no longer sufficient. In order to conserve mass and heat, the necessary explicit horizontal diffusion must be fourth order.

The use of nonhydrostatic drag (Salmon 1986, 1990) or Laplacian horizontal momentum diffusion (Colin de Verdiere 1988, 1989) both require the solution of elliptic equations for each baroclinic mode at each time step, and consequently their computational demand is comparable to that of the primitive equations. In contrast, the present hydrostatic form requires an elliptic solution only for the barotropic pressure (which need only be solved once if the forcing is steady and the bottom flat); the baroclinic pressure is obtained from the temperature by a vertical integration of the hydrostatic relation. These equations are therefore approximately an order of magnitude more computationally efficient. If the biharmonic diffusion were the factor that limited the maximum stable time step, then reducing the grid size by a factor δ_x at fixed λ would require the time step to be reduced by the factor $\delta_t \sim \delta_x^4$, which could substantially increase the computational burden. However, the values of λ and κ_h may be reduced with higher resolution: since the boundary-layer scale depends on the ratio λ/κ_h, λ may evidently be kept small enough to prevent this, with adequate resolution of the boundary layers.

Despite the additional (biharmonic) horizontal diffusive term, the net horizontal diffusive flux across isopycnal surfaces, which arises entirely from the need to smooth the solution and is identically zero in the original equations (1.5′), may (paradoxically) be kept smaller than in level-coordinate primitive equation solutions on similar grids with only Laplacian horizontal diffusion, for two reasons. First, the horizontal diffusivities required for numerical stability are at least an order of magnitude smaller than for the primitive equations, because the mesoscale waves and instabilities have been filtered out by the planetary geostrophic approximation, while the short-wave limit of the planetary geostrophic baroclinic instability spectrum is efficiently damped by the weak horizontal diffusion. Second, as argued above, the combination of Laplacian and biharmonic horizontal diffusion terms allows an approximately adiabatic western boundary layer, since the choice $\lambda = (\epsilon/\beta)^2\kappa_h$ results in a local balance of countergradient and downgradient horizontal diffusive fluxes in the western boundary layer. As long as the net diffusive transport is not countergradient, the biharmonic diffusion is consistent with general thermodynamic constraints. Thus, κ_v and κ_h should be kept large enough to ensure this in general.

7. Summary

A simple friction and diffusion scheme is proposed for solution of the planetary geostrophic equations in a closed basin. The resulting system of Eqs. (2.1)–(2.5) is formally a minor modification of several planetary geostrophic systems that have recently been proposed. However, it has an important advantage over the others: it both admits conditions on normal flow and normal heat flux at rigid boundaries, and is amenable to efficient numerical solution. Solutions of these equations closely resemble solutions of the planetary geostrophic system of Salmon (1990), indicating that the choice of the precise form of the diffusion scheme does not determine the character of the interior flow. However, the computational demand of the equations is considerably less than that of the planetary geostrophic equations of Salmon or Colin de Verdiere (1988, 1989), which require the solution of a three-dimensional elliptic equation at each time step. Because the system is based on the planetary geostrophic equations, it contains only one prognostic field (two in the thermohaline case), no motions with fast timescales, and is of minimal differential order. Consequently, it should also be relatively more amenable to analytic study than, for example, the primitive equations. In work reported elsewhere, we investigate the thermocline structure that arises in solutions of these equations in a closed basin, in the limit of small diapycnal diffusivity (Samelson and Vallis 1997).

Acknowledgments. We are grateful for conversations with J. Pedlosky, M. Spall, R. de Szoeke, and A. Bennett. Comments from anonymous reviewers led to substantial improvements in the presentation. This research was supported for RMS by the National Science Foundation (Grants OCE91-14977 and OCE94-15512), the Office of Naval Research (Grant N00014-92-J-1589), and the Woods Hole Oceanographic Institution, and for GKV by the Office of Naval Research (Grant N00014-94-1-0080) and the National Science Foundation (Grant ATM 93-9317485 and OCE94-15512).

APPENDIX

Differential Order of Linearized Equations

In this appendix we list the leading-order terms of (3.9) for various choices of zero or positive values for the parameters, corresponding to various different proposed friction and diffusion schemes. The number of boundary conditions satisfied by T for various values of the parameters may be deduced by inspection of the leading order term. If $\kappa_v > 0$, the equation is always fourth order in z. With $\epsilon > 0$, the order in x and y depends on the parameters r, κ_h, λ, and G.

Form A

Hydrostatic–biharmonic diffusive: $\epsilon > 0$, $r = 0$, $\kappa_h > 0$, $\kappa_v > 0$, $\lambda > 0$, $\mu = 0$.

At leading differential order,

$$\mathcal{D}(T) \sim -\lambda\Delta_h^2 T_{zz} + \kappa_v T_{zzzz}; \tag{A.1}$$

$\mathcal{D}$ is fourth order in x and y, and fourth order in z (and not strictly elliptic, because of the mixed order of the leading terms). This is the only case that both retains hydrostasy ($r = 0$) and allows boundary conditions on normal velocity and normal heat flux to be specified independently at each boundary. This freedom arises at the lateral boundaries because the biharmonic diffusion decouples the normal gradient of temperature at the boundary from the normal diffusive flux, so that the no-normal-flow and no-heat-flux conditions (2.9) and (2.10) may be applied independently. This is the new formulation that we propose.

Form B

Nonhydrostatic–diffusive: $\epsilon > 0$, $r > 0$, $\kappa_h > 0$, $\kappa_v > 0$, $\lambda = 0$, $\mu = 0$.

At leading differential order,

$$\mathcal{D}(T) \sim r\epsilon\gamma\Delta_h(\kappa_h\Delta_h T + \kappa_v T_{zz}) + \kappa_h\Delta_h T_{zz} + \kappa_v T_{zzzz}, \tag{A.2}$$

so $\mathcal{D}$ is fourth order in x, y, and z (and uniformly strongly elliptic). Normal velocity and thermal boundary conditions may be specified at each boundary. For example, an Ekman pumping and fixed temperature at the surface, and no-normal flow and no flux at all other boundaries, may be specified. This is one of only two cases (the other is **form A**) that allows boundary conditions on velocity and temperature to be specified independently at each boundary. This freedom arises at the lateral boundaries because in the vertical momentum equation the temperature is decoupled from pressure through the presence of the nonhydrostatic term so that the no-normal-flow and no-flux conditions may be applied independently to the pressure and temperature, respectively. This formulation also allows arbitrary forcing terms to be added to the momentum and thermodynamic equations. Salmon (1990) solves the time-dependent nonlinear equations in this form.

Form C

Nonhydrostatic–nondiffusive: $\epsilon > 0$, $r > 0$, $\kappa_h = 0$, $\kappa_v = 0$, $\lambda = 0$, $\mu > 0$.

At leading differential order,

$$\mathcal{D}(T) \sim -(G + rk)\epsilon\gamma\Delta_h T - \mu T_{zz}; \tag{A.3}$$

$\mathcal{D}$ is second order in x, y, and z (and uniformly strongly elliptic). The no-normal-flow condition may be imposed at lateral boundaries, and there is no horizontal heat diffusion, so there is no diffusive heat flux through the boundaries. As in **form B**, nonhydrostatic boundary layers occur. Note that if the stratification G does not vanish, the form of the leading order terms is unchanged in this case if $r = 0$, that is, if hydrostasy is retained. This is not true in **B.** Salmon (1986) solves the steady

linear equations in this form as a prelude to solving the nonlinear equations in **form B**.

Form D

Hydrostatic–harmonic diffusive: $\epsilon > 0$, $r = 0$, $\kappa_h > 0$, $\kappa_v > 0$, $\lambda = 0$, $\mu = 0$.

At leading differential order,

$$\mathcal{D}(T) \sim \kappa_h \Delta_h T_{zz} + \kappa_v T_{zzzz} - G\epsilon\gamma\Delta_h T; \qquad \text{(A.4)}$$

$\mathcal{D}$ is second order in x and y, and fourth order in z (and not elliptic, because of the mixed orders). Since $r = 0$, this form retains hydrostasy. Normal velocity and thermal boundary conditions may still be specified at top and bottom, but only one of these at lateral boundaries. For example, no-normal-flow at lateral boundaries may be specified, but a diffusive heat flux through the boundaries must then be allowed. This flux is generally of order κ_h/ϵ and so not negligible. The situation is unchanged in this case if $G = 0$, that is, if the stratification vanishes. Zhang et al. (1992) and the layer model of Killworth (1985) use essentially this formulation but impose boundary conditions of no-slip on the velocity field and no-diffusive flux on temperature (and salinity). As Killworth (1985) and Zhang et al. (1992) conjecture and the above analysis demonstrates, this is an ill-posed (overdetermined) formulation and is presumably the source of the numerical instability and lack of convergence with increasing resolution that arise in numerical solutions of those two models. Zhang et al. (1992) also suggest a modified set of equations in which ϵ is nonzero for the barotropic mode and zero for the baroclinic modes, but this set is similarly ill-posed even for the free-slip boundary conditions (no-normal-flow and no-normal-flux), since the horizontal differential order of (A.4) is unchanged, and the two boundary conditions do not degenerate to a single condition, when $\epsilon = 0$.

Form E

Hydrostatic–nondiffusive: $\epsilon > 0$, $r = 0$, $\kappa_h = 0$, $\kappa_v > 0$, $\lambda = 0$, $\mu = 0$.

At leading differential order,

$$\mathcal{D}(T) \sim \kappa_v T_{zzzz} - G\epsilon\gamma\Delta_h T; \qquad \text{(A.5)}$$

$\mathcal{D}$ is again fourth order in z, but now the order in x and y depends on the stratification G. If $G > 0$, then $\mathcal{D}$ is second order in x and y, and the situation for the lateral boundaries is essentially as in **form C**, since there is no horizontal heat diffusion. However, if $G = 0$, all derivatives in x and y vanish from $\mathcal{D}$ (since they vanish from $\mathcal{L}$), and the solutions of the corresponding linear equations cannot satisfy any lateral boundary conditions. Since the boundary layer width will depend on G, this form is evidently not workable unless $G > G_0$ can be guaranteed, where for numerical solution G_0 is large enough that the resulting boundary layers are resolved. This difficulty is not due to the degeneracy of the linearization when $G = 0$, but rather to the fact that the evolution equation for T may in that case be solved up to and along the boundary, as the argument given in (3.1)–(3.3) shows.

REFERENCES

Bryan, K., 1969: A numerical method for the study of the circulation of the World Ocean. *J. Comput. Phys.*, **4**, 347–376.

Colin de Verdiere, A., 1986: On mean flow instabilities within the planetary geostrophic equations. *J. Phys. Oceanogr.*, **16,** 1981–1984.

——, 1988: Buoyancy driven planetary flows. *J. Mar. Res.*, **46,** 215–265.

——, 1989: On the interaction of wind and buoyancy driven gyres. *J. Mar. Res.*, **47,** 595–633.

Cox, M., 1985: An eddy-resolving model of the ventilated thermocline. *J. Phys. Oceanogr.*, **15,** 1312–1324.

Huang, R. X., 1988: On boundary value problems of the ideal-fluid thermocline. *J. Phys. Oceanogr.*, **18,** 619–641.

Killworth, P. D., 1985: A two-level wind and buoyancy driven thermocline model. *J. Phys. Oceanogr.*, **15,** 1414–1432.

Luyten, J., J. Pedlosky, and H. Stommel, 1983: The ventilated thermocline. *J. Phys. Oceanogr.*, **13,** 292–309.

Needler, G. T., 1967: A model for thermohaline circulation in an ocean of finite depth. *J. Mar. Res.*, **25,** 329–342.

Pedlosky, J., 1984: The equations for geostrophic motion in the ocean. *J. Phys. Oceanogr.*, **14,** 448–455.

——, 1987: *Geophysical Fluid Dynamics.* Springer, 710 pp.

Phillips, N. A, 1963: Geostrophic motion. *Rev. Geophys.*, **1,** 123–176.

Robinson, A. R., and H. Stommel, 1959: The oceanic thermocline and the associated thermohaline circulation. *Tellus*, **11,** 295–308.

Salmon, R., 1986: A simplified linear ocean circulation theory. *J. Mar. Res.*, **44,** 695–711.

——, 1990: The thermocline as an ''internal boundary layer.'' *J. Mar. Res.*, **48,** 437–469.

Samelson, R. M., and G. K. Vallis, 1997: Large-scale circulation with small diapycnal diffusion: the two-thermocline limit. *J. Mar. Res.*, in press.

Stommel, H., 1948: The westward intensification of wind-driven ocean currents. *Trans. Amer. Geophys. Union*, **99,** 202–206.

——, and J. Webster, 1962: Some properties of thermohaline equations in a subtropical gyre. *J. Mar. Res.*, **20,** 42–56.

Veronis, G., 1975: The role of models in tracer studies. *Numerical Models of the Ocean Circulation,* National Academy of Sciences, Washington, DC, 133–146.

Welander, P., 1959: An advective model of the ocean thermocline. *Tellus*, **11,** 309–318.

——, 1971: Some exact solutions to the equations describing an ideal-fluid thermocline. *J. Mar. Res.*, **21,** 60–68.

Winton, M., and E. Sarachik, 1993: Thermohaline oscillations induced by strong steady salinity forcing of ocean general circulation models. *J. Phys. Oceanogr.*, **23,** 1389–1410.

Zhang, S., C. A. Lin, and R. J. Greatbatch, 1992: A thermocline model for ocean-climate studies. *J. Mar. Res.*, **50,** 99–124.